

MALAYSIAN JOURNAL OF ANALYTICAL SCIENCES

Published by The Malaysian Analytical Sciences Society

ISSN 1394 - 2506

ENHANCED ACTIVITY OF C₃N₄ WITH ADDITION OF ZnO FOR PHOTOCATALYTIC REMOVAL OF PHENOL UNDER VISIBLE LIGHT

(Peningkatan Aktiviti C₃N₄ dengan Penambahan ZnO untuk Fotomangkin Penyingkiran Phenol di bawah Sinaran Tampak)

Faisal Hussin¹, Hendrik O. Lintang², Leny Yuliati²*

¹Department of Chemistry, Faculty of Science, ²Centre for Sustainable Nanomaterials, Ibnu Sina Institute for Scientific and Industrial Research Universiti Teknologi Malaysia, 81310 UTM Johor Bahru, Johor, Malaysia.

*Corresponding author: leny@ibnusina.utm.my

Received: 9 December 2014; Accepted: 3 January 2016

Abstract

Phenol is a stable and hazardous compound that is commonly found as an industrial effluent. Phenol can be treated by photocatalysis using zinc oxide (ZnO) as a photocatalyst. Unfortunately, the use of ZnO in photocatalysis is limited due to the poor response to the visible light. On the other hand, carbon nitride (C_3N_4) is able to absorb visible light. In the present study, a series of ZnO- C_3N_4 was prepared by impregnation method. The effect of zinc to carbon mol ratio (Zn/C) on the properties and photocatalytic activity was examined. X-ray Diffraction (XRD) patterns of the samples revealed that as the Zn mol ratio increased, the intensity of diffraction peaks for ZnO also increased but the intensity for C_3N_4 decreased. All prepared composite materials have an extended absorption band in the visible light region due to the presence of C_3N_4 , as supported by DR UV-Vis spectra. The prepared ZnO- C_3N_4 composites were further investigated in the photocatalytic removal of phenol under visible light for 5 hours. All ZnO- C_3N_4 samples showed higher activity than the bare ZnO with Zn/C mol ratio of 1% showed the highest photocatalytic activity for removal of phenol among all the samples. The high activity observed on the ZnO- C_3N_4 would be due to role of ZnO to suppress electron-hole recombination and C_3N_4 to extend the absorption of ZnO in the visible light region.

Keywords: zinc oxide, carbon nitride, ZnO-C₃N₄ composites, impregnation method, phenol

Abstrak

Fenol adalah sebatian stabil dan berbahaya yang sering dijumpai sebagai efluen industri. Fenol boleh dirawat dengan cara fotopemangkinan menggunakan zink oksida (ZnO) sebagai fotomangkin. Malangnya, penggunaan ZnO di dalam fotopemangkinan adalah terhad disebabkan sedikit respons terhadap sinaran tampak. Sebaliknya, karbon nitrida (C_3N_4) mampu menyerap sinaran tampak. Dalam kajian ini, siri ZnO- C_3N_4 telah disediakan melalui kaedah pengisitepuan. Kesan nisbah mol zink kepada karbon (Zn/C) kepada ciri dan aktiviti fotomangkin telah diperiksa. Corak pembelauan sinar-x (XRD) daripada sampel – sampel membuktikan bahawa kesan nisbah mol Zn meningkat, keamatan puncak pembelauan untuk ZnO semakin naik tetapi keamatan untuk C_3N_4 semakin kurang. Semua bahan komposit yang disediakan mampu memperluaskan jalur penyerapan di dalam kawasan sinaran tampak disebabkan kehadiran C_3N_4 dan disokong oleh spectrum DR UV-Vis. Komposit ZnO- C_3N_4 yang disediakan selanjutnya dikaji di dalam fotomangkin penyerapan ziran fenol di bawah sinaran tampak selama 5 jam. Kesemua sampel ZnO- C_3N_4 mempunyai aktiviti yang tinggi barbanding yang dilihat terhadap ZnO- C_3N_4 berkemungkinan disebabkan peranan ZnO untuk membantutkan penggabungan semula lubang elektron dan C_3N_4 untuk memperluaskan penyerapan ZnO di dalam kawasan sinaran tampak.

Kata kunci: zink oksida, karbon nitrida, komposit ZnO-C₃N₄, kaedah pengisitepuan, fenol

Introduction

Zinc oxide (ZnO) is one of the crucial multifunctional oxide materials for various applications, such as in sensors, solar cells and photocatalysis [1-9]. The ZnO has been investigated due to its unique property of wide band gap (3.37 eV), excitation binding energy (60 meV) at room temperature and good activity for photocatalytic decomposition reactions. Unfortunately, since ZnO has wide band gap and absorption only in the UV region [10], it requires large amount of energy in order to be active as a photocatalyst.

There are various ways to extend the absorption of ZnO to the visible light, such as by incorporating the ZnO with transition metal doping [11 –13], dye sensitizer [14 –15], and CdS [16]. Another feasible modifier is metal free graphitic carbon nitride (C_3N_4) . The C_3N_4 has relatively lower band gap energy (2.70 eV) compared to the ZnO (3.37 eV), thus it is also able to absorb visible light region. Furthermore, the C_3N_4 has a strong covalent bond between carbon and nitrogen in the structure that makes it exhibit high stability under visible light irradiation, which can prevent photocorrosion effect that lead to the decreasing of activity. Due to these unique features, C_3N_4 is used as a visible light driven photocatalyst and it can be combined with other photocatalysts for better photocatalytic activity in the complete spectral region [17]. However, only few reports emphasizing on the incorporation of ZnO with the C_3N_4 . It was reported that the modification of ZnO with C_3N_4 gave a promising result in the photocatalytic removal of methylene blue under visible light irradiation [18].

In this study, phenol was used as the model for organic pollutant. Phenol is considered as a toxic compound released from the industrial as an effluent. Moreover, phenol is very stable and it will remain in the waste water for a long term [19, 20]. Photocatalytic process is one of the available methods that offer both sustainable energy source and environmental friendly process. Since photocatalytic process involves minimum requirement of energy for decomposition of organic pollutant, it is believed that photocatalytic reaction is a green method for phenol decomposition. Moreover, it provides the possibility to utilize the solar light. Therefore, in this study, photocatalytic removal of phenol was investigated by applying visible light over the $ZnO-C_3N_4$ photocatalysts.

Materials and Methods

Preparation of carbon nitride (C₃N₄)

Urea (CO(NH₂)₂, Merck, 99.5%) was used as a source of carbon and nitrogen for preparation of the C_3N_4 . The urea (300 g) was calcined under air atmosphere at a rate of 2.2 °C min⁻¹ for 4 h in order to reach a temperature of 550 °C and tempered for 4 h at this temperature. The resulting yellow solid was ground before using it as the photocatalyst.



Preparation of ZnO

Zinc acetate dihydrate (Zn(CH₃COO)₂.2H₂O, CB; COO)₂.5%) was used as the precursor to synthesize the ZnO. The Zn(CH₃COO)₂.2H₂O (15 g) was calcined 550 at the control of the

Preparation of ZnO-C₃N₄

Various ZnO- C_3N_4 samples were prepared by impregnation method with percentage (mol%). The samples were labelled as ZnO- C_3N_4 (x) with two two sthe ratio of zinc presence the sample. For a typical synthesis of ZnO- C_3N_4 (1), Zn(CH₃COO)₂.2H₂O (0.0716 g) was dissolved in methanol (20 mL). The C_3N_4 (1 g) was then added slowly into the solution, stirred and dried at 30 on a hot plate until drying. The powder was then calcined at 550 °C for 4 h and tempered for 4 h, consecutively

Characterizations

X-ray Diffraction (XRD, Bruker AXS Diffrac plus release 2000) was used to identify the structure of the prepared photocatalysts. The X-ray diffractogram of the catalyst was analyzed at 2θ range of 5-75° with scan rate of 0.05° s⁻¹. Diffuse reflectance Ultraviolet-Visible (DR UV-Vis, Shimadzu UV-2600) spectroscopy was used for measurement of absorption spectra of the prepared photocatalysts. Barium sulphate (BaSO₄) was used as the background reference with the scan range of 200-800 nm. Nicolet iS50 Thermo Scientific Fourier Transform Infrared Spectroscopy (FTIR) was used to detect the presence of functional groups in the composites. The measured wavenumber was in the range of 4000-400 cm⁻¹ with the scan number of 32. Fluorescence spectroscopy (JASCO

Spectrofluorometer FP-8500) was used to obtain emission spectra of samples. The monitored wavelength was in the range of 200-600 nm. Potentiostat/Galvanostat/ZRA (Gamry Instruments Interface 100) was used for the photoelectrochemical studies. Typically, 0.01 g of C_3N_4 , ZnO or ZnO- C_3N_4 composite was added to the solution containing of water (10 mL) and nafion (10 μ L). Then, the solution was sonicated for 10 min. Afterward, the prepared sample (20 μ L) was deposited onto the screen printed electrode (SPE) and then dried using a dryer for 10 min. Na₂SO₄ (0.01 M) and K₃[Fe(CN)₆] (2.5 mM) aqueous solution was employed as an electrolyte. Before measurement, the prepared SPE was immersed in the electrolyte solution (6 mL) and the electrochemical impedance studies were conducted.

Photocatalytic activity test

The photocatalytic removal of phenol was conducted at room temperature. The photocatalyst (0.05 g) was dispersed in 100 mL of jacketed-beaker containing of phenol (50 ppm, 50 mL). Then, the beaker was placed on a stirring plate with cooling water system in a closed box for 30 minutes to let the adsorption reach the equilibrium. The reaction was carried out for 5 hours under visible light irradiation $(150 \text{ W}, \lambda > 400 \text{ nm}, \text{ intensity of } 100,000 \text{ lux})$. After reaction, the solution was taken and separated from the photocatalyst. The remaining phenol was measured by Gas Chromatography equipped with Flame Ionization Detector (GC-FID, Agilent 7820A).

Results and Discussion

Properties of C₃N₄, ZnO and ZnO-C₃N₄

In order to reveal the structure of the prepared samples, the diffraction patterns of the samples were recorded. As can be seen from Figure 1(a), the prepared C_3N_4 showed one intense peak at 2θ of 27.65°, which can be assigned as interlayer distances (d) of 0.32 nm, corresponding to the graphite-like C_3N_4 layer. An additional broad diffraction peak at 2θ of 12.95° with a d value of 0.683 nm showed a hole-to-hole distance of nitride pores, reflecting the geometric effect in pore walls of the prepared C_3N_4 sample [21]. The d values were obtained from the Bragg's law as shown in Equation 1.

 $n\lambda = 2d \sin \theta$ (1)

is a positive integer. The wavelength of the incident wave d is the interplanar distance and d the incident wave d is the interplanar distance.

where n is a positive integer, the wavelength of the incident wave, d is the interplanar distance, and the scattering angle. The presence of these diffraction peaks suggested that the C_3N_4 was prepared successfully. As can been observed from Figure 1(g), the diffraction peaks of the prepared ZnO can be indexed as a wurtzite structure, according to JCPDS file (JCPDS 89-1397).

For the ZnO- C_3N_4 composite samples, there were different trends of the diffraction peaks. For samples with low amount of ZnO (1 – 10 mol %), the samples showed the similar pattern as C_3N_4 with dominant peak at 2θ of 27.75° , suggesting the presence of C_3N_4 in these samples (Figure 1(b)-(c) on the other hand, the samples with high amount of ZnO (20-50 mol %) showed similar diffraction patterns to the ZnO sample. This was reasonable as the amount of ZnO was larger than the C_3N_4 . With the increase of the ZnO, the peak intensity of the C_3N_4 decreased. The XRD patterns clearly showed that the C_3N_4 and ZnO can be detected on the ZnO- C_3N_4 composite samples, depending on the amount of C_3N_4 and ZnO.

Figure 2 shows DR UV-Vis spectra for the ZnO and ZnO- C_3N_4 samples. For the C_3N_4 sample, it showed three strong absorption peaks at 277, 330 and 370 nm, corresponding to the N=C groups of aromatic 1,3,5-triazine, uncondensed C=O group and the terminal N-C group of C_3N_4 , respectively (Fig. 2(a)). It was obvious that the C_3N_4 sample absorbed visible light up to ca. 450 nm. On the other hand, ZnO sample showed one absorption band centered at 320 nm due to the electron charge transfer in the Zn-O linkage, as shown in Fig. 2(g). For the ZnO- C_3N_4 samples, all samples showed the absorption peaks of both C_3N_4 and ZnO (Fig. 2(b)-(f)). As the mol ratio of Zn/C decreased absorption edge of the samples showed blue-shifting from ca. 450 to ca. 380 nm. This was reasonable since when the amount of ZnO increased, the samples would behave like the ZnO, thus giving absorption spectra that were similar to that of the ZnO. From the DR UV-Vis measurements, it can be concluded that ZnO- C_3N_4 samples were successfully synthesized.

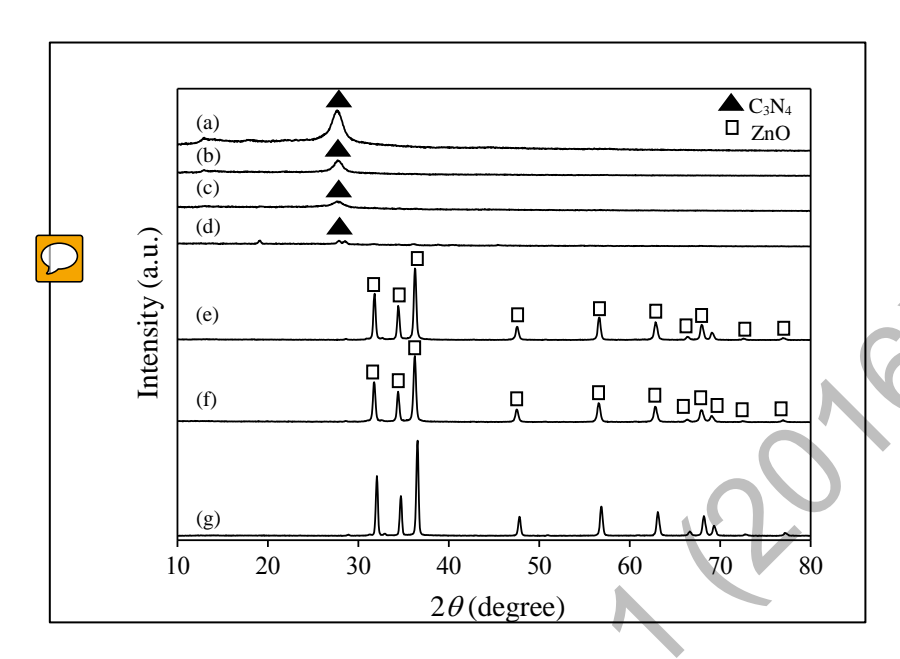


Figure 1. XRD patterns of (a) C_3N_4 , (b) $ZnO-C_3N_4$ (1), (c) $ZnO-C_3N_4$ (5), (d) $ZnO-C_3N_4$ (10), (e) $ZnO-C_3N_4$ (20), (f) $ZnO-C_3N_4$ (50), and (g) ZnO.

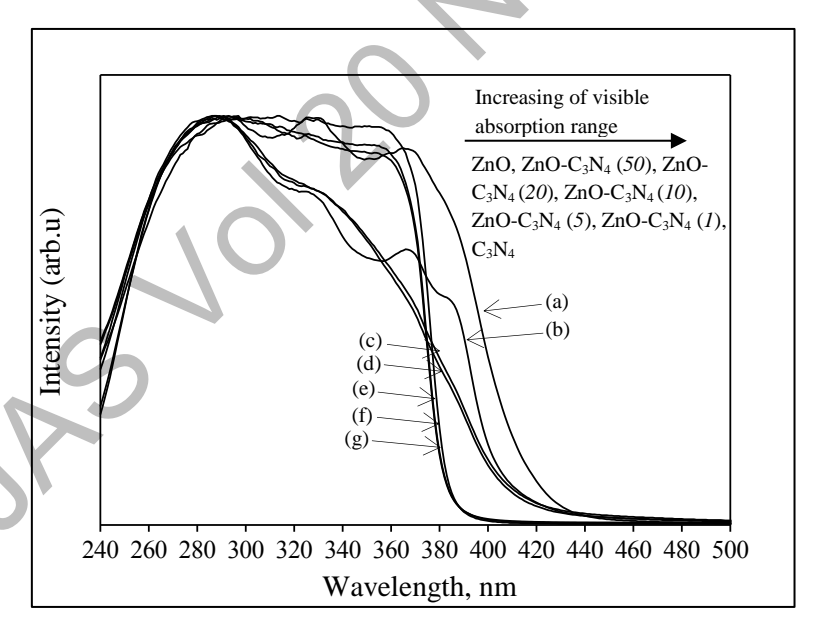


Figure 2. DR-UV Vis spectra of (a) C_3N_4 , (b) $ZnO-C_3N_4$ (1), (c) $ZnO-C_3N_4$ (5), (d) $ZnO-C_3N_4$ (10), (e) $ZnO-C_3N_4$ (20), (f) $ZnO-C_3N_4$ (50), and (g) ZnO.

Figure 3 shows the FTIR spectra of C_3N_4 , ZnO, and ZnO- C_3N_4 samples. As shown in Figure 3(a), the C_3N_4 showed several peaks due to the vibrations of some bondings occurred between carbon and nitrogen. The absorption peak at 810 cm⁻¹ corresponded to the triazine unit of C_3N_4 , while peaks at 1200 -1600 1 region corresponded to stretching modes of C-N heterocyclics. The absorption peaks at 1340 and 1640 cm⁻¹ were related to the C-N and

C=N stretching modes. The broad absorption band at $3100 - 3300 \text{ cm}^{-1}$ can be assigned as primary and secondary amines with their intermolecular hydrogen bonding interactions. All the observed peaks in the FTIR spectrum of C_3N_4 were similar to the absorption peaks reported previously [22-24], supporting the successful transformation of the urea precursor to the C_3N_4 . The prepared ZnO showed an intense peak in the range of $400 - 500 \text{ cm}^{-1}$ (Figure 3(g)), which was belonged to the Zn-O stretching. The FTIR spectra of the prepared ZnO- C_3N_4 samples are shown in Figure 3 (b)-(f). Similar to the results of XRD patterns and DR UV-Vis spectra, samples with low loading of ZnO showed the absorption peaks of C_3N_4 as the dominant species. The peaks assigned to the C_3N_4 decreased with the increase of Zn/C ratio. When the Zn/C ratio reached 50 mol%, the peaks related to the C_3N_4 were completely disappeared and only ZnO peak could be observed on the ZnO- C_3N_4 (50) sample, as shown in Figure 3(f).

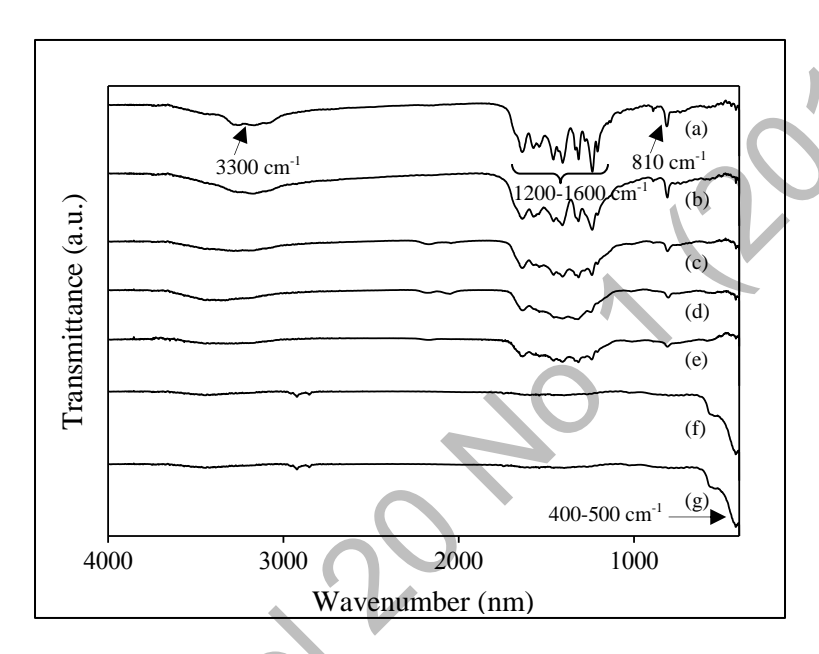


Figure 3. FTIR spectra of (a) C_3N_4 , (b) $ZnO-C_3N_4$ (1), (c) $ZnO-C_3N_4$ (5), (d) $ZnO-C_3N_4$ (10), (e) $ZnO-C_3N_4$ (20), (f) $ZnO-C_3N_4$ (50), and (g) ZnO

Since the activity of the $ZnO-C_3N_4$ samples were evaluated under visible light irradiation, the charge transfer mechanism was investigated from the C_3N_4 site. The C_3N_4 exhibited two excitation peaks around 277 and 370 nm The excitation peaks at 277 nm would be related to the N=C groups of aromatic 1,3,5-triazine, while the peak of 370 nm would be due to the terminal N-C group of C_3N_4 [14, 22]. In order to investigate the effect of addition of ZnO on the emission of the C_3N_4 , the emission spectra of the C_3N_4 and the ZnO- C_3N_4 samples were measured at the excitation wavelength of 277 and 370 nm, as shown in Figure 4. For both excitation wavelengths, the C_3N_4 showed two emission sites at 445 and 460 nm (Figure 4(a)). The emission intensity was found to decrease with the addition of ZnO (Figig (Figure 4(b)-(f))). The higher the amount of Zn/C ratio, the lower the emission intensity of the ZnO- C_3N_4 samples obtained. This result clearly suggested that there were interactions between the emission sites of C_3N_4 and the added ZnO particles. Since the emission is the result of electron-hole recombination, the low emission intensity would suggest the suppression of the electron-hole recombination. It can be proposed here that the addition of ZnO was able to suppress the electron-hole recombination of the C_3N_4 . Therefore, under visible light irradiation, it can be suggested that the electrons from the conduction band of the C_3N_4 would be trapped by the ZnO, which would cause the less electron-hole recombination process. The mechanism of the electron charge transfer can be illustrated as in Figure 5.

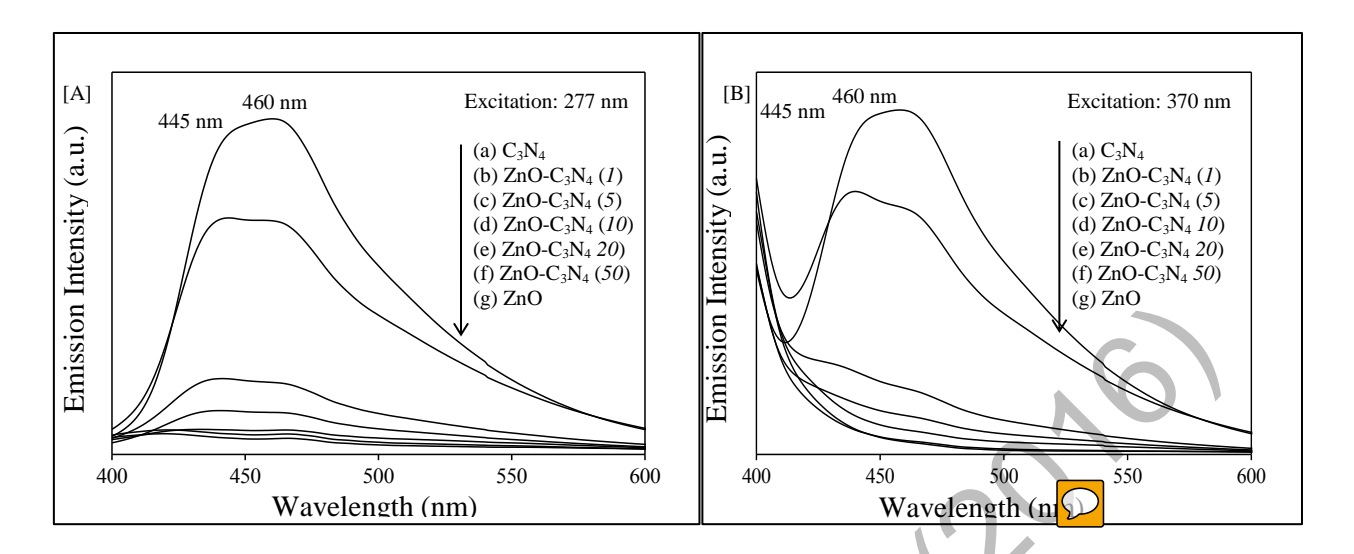


Figure 4. Emission spectra of (a) C_3N_4 , (b) $ZnO-C_3N_4$ (1), (c) $ZnO-C_3N_4$ (5), (d) $ZnO-C_3N_4$ (10), (e) $ZnO-C_3N_4$ (20), (f) $ZnO-C_3N_4$ (50) and (g) ZnO monitored at the excitation wavelength of [A] 277 and [B] 370 nm.

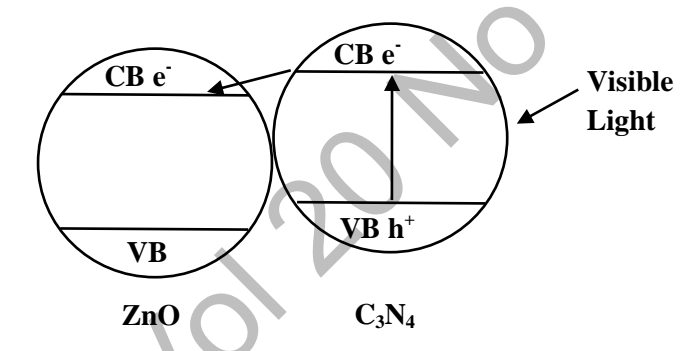


Figure 5. Schematic illustration of the electron charge transfer in the ZnO-C₃N₄ composite. CB and VB are conduction and valence bands, respectively.

In addition to the reduced electron-hole recombination, the lower emission intensity especially for samples with high loading of ZnO would be also caused by the smaller amount of the C_3N_4 . This factor would also affect the photocatalytic activity of the ZnO- C_3N_4 composites under visible light irradiation.

Photocatalytic activity test

The C_3N_4 , ZnO, and the ZnO- C_3N_4 samples were evaluated for the photocatchetic removal of phenol. Table 1 shows the percentage removals of phenol on the samples. The C_3N_4 showed 34% moval of phenol (Entry 1), while the ZnO showed 15% (Entry 7). The ZnO $_3N_4$ (I) showed 43% removal of phenol, which was three times higher than the activity of ZnO alone (Entry 7) is worthy noted that the ZnO- C_3N_4 (I) showed higher activity than either C_3N_4 or ZnO. This result showed that there was a synergetic effect between the small amount of ZnO and the C_3N_4 . As discussed previously, the small amount of ZnO would act to trap electron, thus inhibiting the electron-hole recombination process in the C_3N_4 sample. The less electron-hole recombination would be the key factor to get the improved photocatalytic activity.

Unfortunately, when the Zn ratio was more than 1 mol%, the activity was found to be gradually decreased with the increase of the Zn ratio (Entries 3-6). Therefore, the ZnO-C₃N₄ (I) showed the highest activity among the composite samples. As shown in the DR UV-Visible spectra, the ZnO-C₃N₄ (I) showed the most intense absorption in the visible light. This property would be also one of the parameters that made it superior among the other composites. Moreover, as discussed in the characterization parts, samples with low loading of ZnO would behave like C₃N₄, while samples with high loading among would behave like ZnO. The ZnO-C₃N₄ (50) showed activity closer to the activity of the ZnO (Entries 6 and 7). Even though the activity decreased with the increase of the ZnO loading it is clear that all ZnO-C₃N₄ composites showed better activities than the unmodified ZnO. This result strongly gested that the activity of C₃N₄ can be increased by the addition of ZnO.

Table 1. The percentages of phenol removal on ZnO and ZnO-C₃N₄ samples after 5 hours reaction under visible light irradiation^a

Entry	Samples	Percentage of phenol removal (%) ^b
1	C_3N_4	32
2	$ZnO-C_3N_4(1)$	43
3	$ZnO-C_3N_4$ (5)	34
4	$ZnO-C_3N_4$ (10)	33
5	ZnO-C ₃ N ₄ (20)	26
6	$ZnO-C_3N_4$ (50)	21
7	ZnO	15

^aPhotocatalyst used was 0.05 g in the 50 mL solution of phenol (50 ppm)

^bPercentage removal of phenol was calculated from the percentage ratio of reacted phenol to the initial concentration of phenol

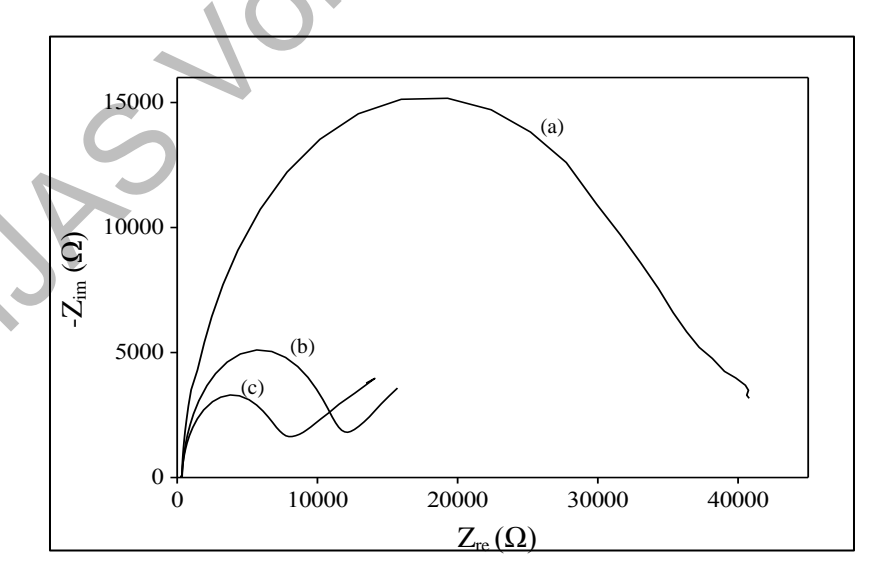


Figure 6. Nyquist plots of (a) ZnO, (b) C_3N_4 , and (c) ZnO- C_3N_4 (1).

Faisal et al: ENHANCED ACTIVITY OF C_3N_4 WITH ADDITION OF ZnO FOR PHOTOCATALYTIC REMOVAL OF PHENOL UNDER VISIBLE LIGHT

In order to obtain more detail information on the charge transfer and further support the synergetic effect between the ZnO and the C_3N_4 , the electrochemical impedance measurement was carried out. Nyquist plots of the C_3N_4 , the ZnO and the ZnO- C_3N_4 (1) composite were plotted with an open circuit between 1 MHz and 0.1 Hz as shown in Figure 6. The ZnO- C_3N_4 (1) composite showed smaller semicircles compare to the bare ZnO and the C_3N_4 , indicating the lower charge-transfer resistance on the surface of the composite [25]. With the suitable amount of ZnO, the charge transfer increased since C_3N_4 can transfer the electron to the ZnO thus, preventing the rapid electron-hole recombination. This synergetic effect resulted in the higher activity in the photocatalytic reaction.

Conclusion

The ZnO- C_3N_4 samples were prepared successfully by impregnation method. All the ZnO- C_3N_4 samples showed higher activity than the bare ZnO. The optimum amount of 1 mol% of Zn ratio gave ca. 3 times higher activity than unmodified ZnO. The ZnO- C_3N_4 (I) also showed higher activity than the C_3N_4 . The synergic effect between the C_3N_4 and the ZnO was proposed, where the addition of C_3N_4 was able to extend the absorption of ZnO to visible light region and the small amount of ZnO would act to trap electron and suppress the electron-hole recombination.

Acknowledgement

This work was financially supported by the Ministry of Higher Education (MOHE, Malaysia) and the Universiti Teknologi Malaysia (UTM, Malaysia) through a Tier-1 Research University Grant (cost center code: Q.J130000.2509.06H66). F. H acknowledges the support of UTM through Zamalah Scholarships.

References

- 1. Wang, L., Kang, Y., Lui, X., Zhang, S., Huang, W. and Wang, S. (2012). ZnO Nanorod Gas Sensor for Ethanol Detection. *Sensors Actuators B: Chemical*, 162 (1): 237 243.
- 2. Wang, W., Huang, H., Li, Z., Zhang, H., Wang, Y., Zheng, W. and Wang, C. (2008). Zinc Oxide Nanofibers Gas Sensor via Electrospinning. *Journal of the American Ceramic Society*, 91 (11): 3817 3819.
- 3. Jean, J., Chang, S., Brown, P. R., Cheng, J. J., Rekemeyer, P. H., Bawendi, M. G., Gradečak, S. and Bulović, V. (2013). ZnO Nanowire Arrays for Enhanced Photocurrent in PbS Quantum Dot Solar Cells. *Advanced Materials*, 25 (20): 2790 2796.
- 4. Zhang, M.-L., Jin, F., Zheng, M.-L., Liu, J., Zhao, Z.-S. and Duan, X.-M. (2014). High Efficiency Solar Cell Based on ZnO Nanowire Array Prepared by Different Growth Methods. *RSC Advances*, 4 (21): 10462 10466.
- 5. Kaur, J., Bansal, S. and Singhal, S. (2013). Photocatalytic Degradation of Methyl Orange Using ZnO Nanopowders Synthesized via Thermal Decomposition of Oxalate Precursor Method. *Physica B: Condensed Matter*, 416: 33 38.
- 6. Kayaci, F., Vempati, S., Donmez, I., Biyikli, N. and Uyar, T. (2014). Role of Zinc Interstitial and Oxygen Vacancies of ZnO in Photocatalysis: A Bottom-up Approach to Control Defect Density. *Nanoscale*, 6 (17): 10224–10234.
- 7. Tian, C., Zhang, Q., Wu, A., Jiang, M., Liang, Z., Jiang, B. and Fu, H. (2012). Cost-Effective Large-Scale Synthesis of ZnO Photocatalysts with Excellent Performance for Dye Photodegradation. Chemical Communication, 48 (23): 2858 2860.
- 8. Kumar, R., Kumar, G. and Umar, A. (2013). ZnO Nano-Mushrooms for Photocatalytic Degradation of Methyl Orange. *Materials Letters*, 97: 100 103.
- 9. Ameen, S., Akhtar, M.S., Nazim, M. and Shin, H.-S. (2013). Rapid Photocatalytic Degradation of Crystal Violet Dye over ZnO Flower Nanomaterials. *Materials Letters*, 96: 228 232.
- 10. Suchanek, W. L. (2009). Systematic Study of Hydrothermal Crystallization of Zinc Oxide (ZnO) Nano-Sized Powders with Superior UV Attenuation. *Journal of Crystal Growth*, 312 (1): 100 108.
- 11. Lu, Y.-H., Lin, W.-H., Yang, C.-Y., Chiu, Y.-H., Pu, Y.-C, Lee, M.-H., Tseng, Y.-C. and Hsu. Y.-J. (2014). A Facile Green Antisolvent Approach to Cu²⁺-Doped ZnO Nanocrytals h Visible-Light Responsive Photoactivities. *Nanoscale*, 6 (15): 8796 8803.
- 12. Li, P., Wei, Z., Wu, T., Peng, Q. and Li, Y. (2011). Au-ZnO Hybrid Nanopyramids and Their Photocatalytic Properties. *Journal of the American Chemical Society*, 133 (15): 5660 5663.
- 13. Chauhan, R., Kumar, A. and Chaudhary, R.P. (2012). Photocatalytic Studies of Silver Doped ZnO Nanoparticles Synthesized by Chemical Precipitation Method. *Journal of Sol-Gel Science Technology*, 63 (3): 546 553.

- 14. Sarkar, S., Makhal, A., Bora, T., Lakhsman, K., Singha, A., Dutta, J. and Pal., S.K. (2012). Hematoporphyrin-ZnO Nanohybrids: Twin Applications in Efficient Visible-Light Photocatalysis and Dye-Sensitized Solar Cells. *ACS Applied Materials & Interfaces*, 4 (12): 7027 7035.
- 15. Yang, G. C. C. and Chan, S.-W. (2009). Photocatalytic Reduction of Chromium (VI) in Aqueous Solution using Dye-Sensitized Nanoscale ZnO under Visible Light Irradiation. *Journal of Nanoparticle Research*, 11 (1): 221 230.
- 16. Zou, X., Wang, P.-P., Li, C., Zhao, J., Wang, D., Asefa, T. and Li, G.-D. (2014). One-Pot Cation Exchange Synthesis of 1D Porous CdS/ZnO Heterostructures for Visible-Light-Driven H₂ Evolution. *Journal of Materials Chemistry A*, 2 (13): 4682 4689.
- 17. Yan, H., Chen, Y. and Xu. S. (2012). Synthesis of Graphitic Carbon-Nitride by Directly Heating Sulfuric Acid Treatment Melamine for Enhanced Photocatalytic H₂ Production from Water Under Visible Light. *International Journal of Hydrogen Energy*, 37 (1): 125 133.
- 18. Wang, Y., Shi, R., Lin, J. and Zhu, Y. (2011). Enhancement of Photocurrent and Photocatalytic Activity of ZnO Hybridized with Graphite-Like C₃N₄. *Energy & Environmental Science*, 4 (8): 2922 2929.
- 19. Pardeshi, S.K. and Patil, A.B. (2008). A Simple Route for Photocatalytic Degradation of Phenol in Aqueous Zinc Oxide Suspension Using Solar Energy. *Solar Energy*, 82 (8): 700 705.
- 20. Ahmed, S., Rasul, M. G, Martens, W. N., Brown, R. and Hashib, M. A. (2010). Heterogeneous Photocatalytic Degradation of Phenols in Wastewater: A Review on Current Status and Developments. *Desalination*, 261(1-2): 3 –18.
- 21. Pang, L.-L., Bi, J.-Q., Bai, Y.-J., Qi, Y.-X., Zhu, H.-L., Wang, C.-G., Wu, J.-W. and Lu, C.-W. (2008). Rapid Synthesis of Graphitic Carbon Nitride Powders by Metathesis Reaction between CaCN₂ and C₂Cl₆. *Materials Chemistry Physics*, 112 (3): 1124 –1128.
- 22. Sam, M. S., Lintang, H. O., Sanagi, M. M., Lee, S.L. and Yuliati, L. (2014). Mesoporous Carbon Nitride for Adsorption and Fluorescence Sensor of N-Nitrosopyrrolidine. *Spectrochimica Acta Part A: Molecular and Bimolecular Spectroscopy*, 124: 357 364.
- 23. Li, X., Zhang, J, Shen, L., Ma, Y., Lei, W., Cui, Q. and Zou, G. (2009). Preparation and Characterization of Graphitic Carbon Nitride through Pyrolysis of Melamine. *Applied Physics A*, 94 (2): 387 392.
- 24. Martha, S., Nashim, A. and Parida, K.M. (2013) Facile Synthesis of Highly Active g-C₃N₄ for Efficient Hydrothermal Production under Visible Light. *Journal of Materials Chemistry A*, 1: 7816 –7824.
- 25. Luo, Q.-P., Yu, X.-Y., Lei, B.-X., Chen, H.-Y., Kuang, D.-B. and Su, C.-Y. (2012). Reduced Graphene-Oxide-Hierarchical ZnO Hollow Sphere Composites with Enhanced Photocurrent and Photocatalytic Activity. *Journal of Physical Chemistry C*, 116: 8111 8117.